Carbenium Ions

DOI: 10.1002/anie.200907015

The *tert*-Butyl Cation in H-Zeolites: Deprotonation to Isobutene and Conversion into Surface Alkoxides**

*Christian Tuma, Torsten Kerber, and Joachim Sauer**

There is continuous interest in the mechanisms of hydrocarbon synthesis and transformation processes using acidic zeolite catalysts. Initially, it was assumed that these reactions follow mechanisms known from chemistry in superacidic media, and involve carbocations as intermediates.[1] However, evidence for persistent carbenium ions has only been produced for cyclic alkenyl or aromatic carbenium ions by NMR,[2] UV/Vis,[3] and IR spectroscopy[4,5] or computational techniques,[6] but not for carbenium ions derived from small alkenes, which rather attach to the surface oxygen sites to form alkoxides.[7–9] Nicholas and Haw concluded that stable carbenium ions in zeolites can be observed by NMR spectroscopy if the parent compound (from which the carbenium ion is obtained by protonation) has a proton affinity of 875 kJ mol^{-1} or larger.[10] Quantum chemical calculations showed that this statement is more general and that proton transfer from a H-zeolite to a molecule[6] or molecular cluster[11] occurs if its proton affinity is about that of ammonia (854 kJ mol^{-1}) or larger.[12]

An obvious candidate for a stable noncyclic carbenium ion is the *tert*-butyl cation observed in superacidic media, even if the proton affinity of isobutene (802 kJ mol^{-1})[13] does not make it very likely that it will exist in zeolites.[12] It may be formed by protonation of isobutene or as intermediate,[14,15] but experimental attempts to produce evidence for either the *tert*-butyl cation or an alkoxide have been unsuccessful to date.[16,17] Several quantum chemical studies have applied standard density functional theory (DFT) to localize stationary points for the *tert*-butyl cation in zeolites.[18–21] However, a proof (vibrational analysis) has only been presented for H-mordenite[20] and H-ferrierite[22] that the cation is indeed a local minimum on the potential energy surface.

According to these calculations, the *tert*-butyl cation **1** shown in Figure 1 is a metastable intermediate with a stability between that of the *tert*-butoxide **2** and the isobutoxide **3**.

It has subsequently been shown[22–24] that reliable energies for hydrocarbon species in zeolites can only be obtained if two problems of currently used density functionals are addressed: dispersion energy contributions to adsorption energies, and self-interaction correction (SIC) errors of gradient-corrected functionals leading to overstabilization of polar structures, such as carbenium ions in zeolites. Based on a hybrid MP2:DFT method[25] that combines second-order Møller–Plesset perturbation theory (MP2) for the reaction site with DFT for the full periodic structure, a multi-step protocol has been designed that yields MP2-quality results for the full periodic structure.[22] Such calculations yield an adsorption energy of 77 kJ mol^{-1} for isobutene in H-ferrierite (H-FER) and predict that the *tert*-butyl carbenium ion (**1**) is 60 kJ mol^{-1} less stable than adsorbed isobutene (**4**) and also 24 and 51 kJ mol^{-1} less stable than *tert*-butoxide (**2**) and isobutoxide (**3**), respectively (Figure 1, right). Nevertheless, **1** may be formed as an intermediate, for example in the skeletal isomerization of butenes[15] or by reacting *tert*-butyl halides with alkaline ion exchanged zeolites.[14] The lifetime will then depend on the barriers separating it from isobutene and the alkoxides.

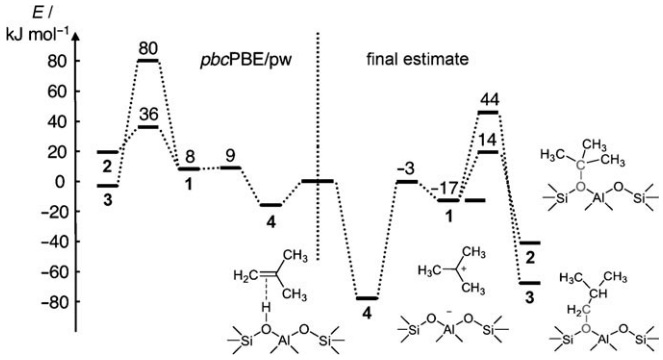

Figure 1. Potential energy surfaces for the isobutene/H-ferrierite system calculated with PBE (left) and with the hybrid MP2:PBE method (final estimate; right).

Herein, we use the hybrid MP2:DFT method[22] to calculate the intrinsic energy barriers $E(i/\mathbf{1}-\mathbf{1})$ for $i = \mathbf{2}, \mathbf{3}, \mathbf{4}$ (Table 1; "final estimate" shows the results together with the reaction energies $E_R(\mathbf{1}-i)$). The lowest barrier is found for the conversion of the *tert*-butyl carbenium ion into isobutene (14 kJ mol^{-1}), whereas barriers of 31 and 61 kJ mol^{-1} have to be surmounted for conversion into isobutoxide and *tert*-butoxide, respectively (Figure 1).

Our calculations adopt the same ferrierite double cell (1897 × 1426 × 1501 pm) as in reference [22], and involve five steps:

1) DFT optimization by applying periodic boundary conditions (pbc) with subsequent frequency calculations for

[*] Dr. C. Tuma, T. Kerber, Prof. Dr. J. Sauer
Humboldt Universität zu Berlin, Institut für Chemie
Unter den Linden 6, 10099 Berlin (Germany)
Fax: (+49) 30-2093-7136
E-mail: sek.qc@chemie.hu-berlin.de

[**] This work has been supported by the Deutsche Forschungsgemeinschaft (priority programme 1155). We also thank the Norddeutscher Verbund für Hoch- und Höchstleistungsrechnen (HLRN) for computing time.

Supporting information for this article, including details of computations, is available on the WWW under http://dx.doi.org/10.1002/anie.200907015.

Table 1: Different contributions to intrinsic energy and enthalpy barriers and to reaction energies and enthalpies [kJ mol^{-1}].[a]

	Energy barriers	4/1−1	2/1−1	3/1−1	1−4	1−2	1−3
1	PBE/pw(pbc)	1.6	28.1	72.1	24.5[b]	−11.7[b]	12.7[b]
2	MP2/TZVP(P):PBE/pw	7.1	12.8	57.0	63.5[b]	52.3[b]	66.7[b]
3	periodic model corr.	−1.8	4.3	−1.2	−2.8	−3.2	2.9
4	CBS corr.	7.1	17.6	3.7	3.6[b]	−22.2[b]	−15.2[b]
5	CCSD(T)−MP2, TZVP, $6T_{9H}$	1.4	−3.3	1.6	−4.1[b]	−3.2[b]	−3.7[b]
6	Final estimate	13.8	31.5	61.1	60.1	23.6	50.7
7	Difference to PBE	12.3	3.3	−11.0	35.6	35.4	38.0
8	ZPVE [PBE/pw(pbc)][c]	3.7	13.1	10.4	−11.8	−21.1	−19.0
9	$H_{298}-E$[PBE/pw(pbc)][d]	−3.6	4.8	3.3	−8.6	−12.4	−15.1

[a] The barriers of the reverse reactions can be calculated as $E^{\ddagger}(i/\mathbf{1}-i) = E^{\ddagger}(i/\mathbf{1}-\mathbf{1}) + E_R(\mathbf{1}-i)$. [b] Values calculated from Ref. [22]. [c] Zero-point vibrational energy. [d] Contribution to enthalpy at 298 K.

stationary points, yielding zero-point vibrational energies (ZPVE) and partition functions. We apply the Perdew–Burke–Ernzerhofer (PBE) functional[26] with plane-wave (pw) basis sets and employ the CPMD code.[27]

2) Reoptimization at the hybrid MP2:PBE level. The energy of the entire system, E(S), is calculated with the same low-level method that was used for step (1), here PBE/pw(pbc). For a finite-size cluster model, C (the $16T_{16H}$ model from Figure 1 in Ref. [22]), two calculations are performed. The first uses the low-level method (PBE/pw) and the other employs MP2 with the TZVP(P) basis set[22] as the high-level method, yielding E_{PBE}(C) and E_{MP2}(C), respectively. Optimization on the hybrid MP2:PBE potential energy surface [Eq. (1)],

$$E_{MP2:PBE}(C:S) = E_{MP2}(C) + E_{PBE}(S) - E_{PBE}(C) \quad (1)$$

employed the QMPOT code[28] interfaced to CPMD[27] for the PBE calculations and to the RICC2 module[29] of TURBOMOLE for the MP2 part.

Figure 2 shows the transition structures **4/1**, **2/1**, and **3/1** thus obtained. Table 2 summarizes relevant bond distances and compares them with those of the stable structures. The distance between the bridging oxygen atom of the Brønsted site and the closest carbon atom is much larger in the π complex **4** and in the cation **1** (292 and 290 pm, respectively) than in the covalently bonded alkoxides **2** and **3** (161 and 151 pm, respectively). In the **4/1** transition structure, this distance is even smaller than in both the intermediates **4** and **1**, whereas the C−C bond distances are between those of structures **4** and **1**. In all transition structures, the C−C bond distances are shortened by up to 14 pm compared to a standard C−C bond length.

3) Calculation of the periodic model correction. The hybrid MP2:PBE energy [Eq. (1)] can be interpreted as a PBE description of the entire system to which a high-level correction for the reaction site is added [Eq. (2)].

$$E_{HL-corr}(C) = E_{MP2}(C) - E_{PBE}(C) \quad (2)$$

This difference shows an asymptotically convergent behavior as a function of the cluster size (see Figure 5c of Ref. [22]), and apart from a constant term (associated with the SIC error of PBE), $E_{HL\text{-}corr}$(C) fits to an atom pair sum of damped $1/R^6$ terms associated with missing dispersion contributions. From the non-transferable parameters obtained, the high-level correction for the full periodic structure, $E_{HL\text{-}corr}$(S), is calculated.[23] The difference [Eq. (3)]

$$E_{HL\text{-}corr}(S) - E_{HL\text{-}corr}(C) \quad (3)$$

defines the periodic model correction, which, when added to $E_{MP2:PBE}$(C:S), yields an estimate for the MP2 energy of the full periodic structure for the basis set used.

For the formation of **1**–**4** and **2/1**, **3/1**, and **4/1** on the zeolite surface from gas-phase isobutene, the values are all between −14 and −21 kJ mol^{-1} (Supporting Information, Table S1, row 3), so that the periodic model corrections for the intrinsic barriers and reaction energies in Table 2 are very small (between −3.2 and +4.3 kJ mol^{-1}). This result means that the dispersion contribution to the binding energy, which is similar for all surface species, dominates the MP2-PBE difference for cluster sizes beyond $C = 16T_{16H}$.

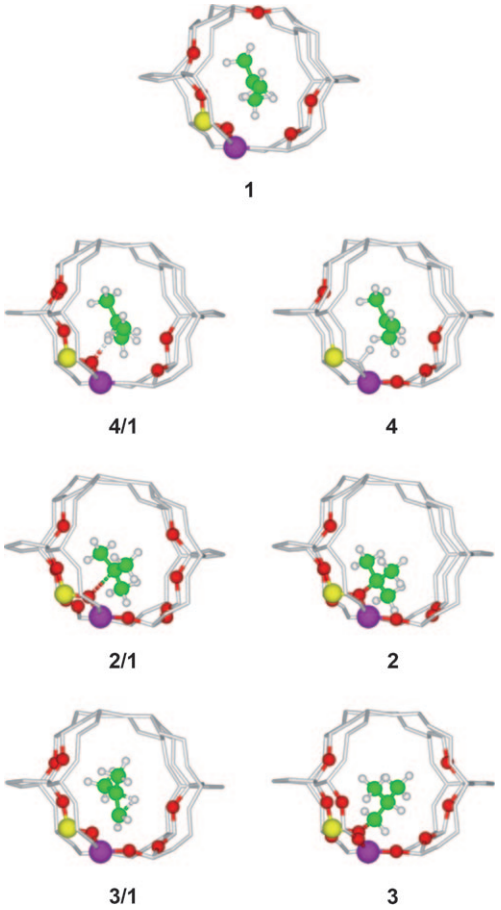

Figure 2. Hybrid MP2:PBE-optimized intermediate and transition structures within the pore of H-FER. Oxygen atoms (red) are closer than 280 pm to any of the hydrocarbon atoms (Si yellow, Al magenta, C green).

Table 2: Distance between the oxygen atom of the zeolitic Brønsted site and the closest carbon atom and C–C bond distances [pm] for the intermediates **1**–**4** and transition structures **4/1**, **2/1**, and **3/1**.

Distance	**1**	**4/1**	**4**	**2/1**	**2**	**3/1**	**3**
O–C	290	285	292	261	161	219	151
C–C	145	140	135	145	151	140	152
	145	147	150	146	152	150	152
	145	147	150	146	152	150	153

4) MP2 energies are corrected for the basis-set superposition error (BSSE) and are extrapolated to the complete basis-set limit. The MP2/CBS corrections vary between 15 and 41 kJ mol^{-1} (Supporting Information, Table S1, row 4) and thus do not cancel when calculating intrinsic barriers and reaction energies.

5) The reliability of MP2 is checked by single-point CCSD(T) calculations (TZVP basis set, $6T_{9H}$ model).[22] The differences are small; in absolute terms, they are 7 kJ mol^{-1} or less for the formation of different surface species (Supporting Information, Table S1, row 5) and 4.1 kJ mol^{-1} or less for intrinsic barriers and reaction energies (Table 1), indicating that MP2 is an excellent approximation for studying protonation and alkoxide formation in zeolites. A similar conclusion was reached for methylation reactions of alkenes in H-zeolites.[24]

Figure 1 shows that the final estimates obtained by our multistep protocol yield a reaction energy profile that deviates significantly from the PBE result. The differences between the final estimates and PBE (Supporting Information, Table S1, row 7) are due to an interplay between missing stabilizing dispersion effects in PBE for all species (making the difference negative) and the presence of stabilizing SIC effects with PBE for polar species such as **1** and the transition structures only. This results in a constant PBE total error for the relative stability of **2**, **3**, and **4** with respect to **1**, whereas the error for the barriers separating **1** from **2**, **3**, and **4** varies between 12 and −11 kJ mol^{-1} (Table 1). We conclude that we cannot expect to get reliable relative stabilities and energy barriers from the computationally efficient PBE + Dispersion approach,[23,30] because the latter corrects for the dispersion error only and not for the SIC error (see Ref. [24]).

As a result, the *tert*-butyl carbenium ion **1** becomes the (thermodynamically) least stable species on the potential energy surface, but the barrier separating it from the most stable adsorbed isobutene **4** increases from 5.2 (PBE) to 17.5 kJ mol^{-1} (including zero-point vibrational contributions) with a remaining uncertainty of ±5 kJ mol^{-1} (near chemical accuracy).[24] This result means that at 298 K, the rate constant k for the conversion of a *tert*-butyl carbenium ion into adsorbed isobutene by proton transfer to the zeolite decreases by more than two orders of magnitude, and the half life $\tau_{1/2} = \ln 2/k$ increases from 0.42 μs to 59 μs, with an estimated uncertainty range of 10–450 μs.[31] For detection by NMR spectroscopy,[16] this is probably not long enough, but the timescale of UV/Vis spectroscopy[17] should in principle allow for the detection of this carbenium ion once it has formed, for example, from *tert*-butyl halides.

Received: December 13, 2009
Published online: May 20, 2010

Keywords: butene · carbenium ions · density functional theory · hydrocarbons · zeolites

[1] P. A. Jacobs in *Carbionogenic Activity of Zeolites*, Elsevier, Amsterdam, **1977**.
[2] J. F. Haw, *Phys. Chem. Chem. Phys.* **2002**, *4*, 5431 – 5441.
[3] M. Bjørgen, F. Bonino, S. Kolboe, K.-P. Lillerud, A. Zecchina, S. Bordiga, *J. Am. Chem. Soc.* **2003**, *125*, 15863 – 15868.
[4] S. Yang, J. N. Kondo, K. Domen, *Chem. Commun.* **2001**, 2008 – 2009.
[5] S. Yang, J. N. Kondo, K. Domen, *Catal. Today* **2002**, *73*, 113 – 125.
[6] L. A. Clark, M. Sierka, J. Sauer, *J. Am. Chem. Soc.* **2003**, *125*, 2136 – 2141.
[7] J. F. Haw, W. Song, D. M. Marcus, J. B. Nicholas, *Acc. Chem. Res.* **2003**, *36*, 317 – 326.
[8] T. Xu, J. Zhang, E. J. Munson, J. F. Haw, *J. Chem. Soc. Chem. Commun.* **1994**, 2733 – 2735.
[9] M. T. Aronson, R. J. Gorte, W. E. Farneth, D. White, *J. Am. Chem. Soc.* **1989**, *111*, 840 – 846.
[10] J. B. Nicholas, J. F. Haw, *J. Am. Chem. Soc.* **1998**, *120*, 11804 – 11805.
[11] V. Termath, F. Haase, J. Sauer, J. Hutter, M. Parrinello, *J. Am. Chem. Soc.* **1998**, *120*, 8512 – 8516.
[12] J. Sauer in *Handbook of Hydrogen Transfer*, *Vol. 2* (Eds.: R. L. Schowen, J. P. Klinman, J. T. Hynes, H.-H. Limbach), Wiley-VCH, Weinheim, **2006**, pp. 685 – 707.
[13] E. P. Hunter, S. G. Lias in *NIST Chemistry WebBook, NIST Standard Reference Database Number 69* (Eds.: P. J. Linstrom, W. G. Mallard), National Institute of Standards and Technology, Gaithersburg MD, 20899, **2005**.
[14] R. J. Corrêa, C. J. A. Mota, *Phys. Chem. Chem. Phys.* **2002**, *4*, 4268 – 4274.
[15] A. Boronat, A. Corma, *Appl. Catal. A* **2008**, *336*, 2 – 10.
[16] N. D. Lazo, B. R. Richardson, P. D. Schettler, J. L. White, E. J. Munson, J. F. Haw, *J. Phys. Chem.* **1991**, *95*, 9420 – 9425.
[17] H. Ishikawa, E. Yoda, J. N. Kondo, F. Wakabayashi, K. Domen, *J. Phys. Chem. B* **1999**, *103*, 5681 – 5686.
[18] P. E. Sinclair, A. de Vries, P. Sherwood, C. R. A. Catlow, R. A. van Santen, *J. Chem. Soc. Faraday Trans.* **1998**, *94*, 3401 – 3408.
[19] X. Rozanska, R. A. van Santen, T. Demuth, F. Hutschka, J. Hafner, *J. Phys. Chem. B* **2003**, *107*, 1309 – 1315.
[20] M. Boronat, P. M. Viruela, A. Corma, *J. Am. Chem. Soc.* **2004**, *126*, 3300 – 3309.
[21] C. Tuma, J. Sauer, *Angew. Chem.* **2005**, *117*, 4847 – 4849; *Angew. Chem. Int. Ed.* **2005**, *44*, 4769 – 4771.
[22] C. Tuma, J. Sauer, *Phys. Chem. Chem. Phys.* **2006**, *8*, 3955 – 3965.
[23] T. Kerber, M. Sierka, J. Sauer, *J. Comput. Chem.* **2008**, *29*, 2088 – 2097.
[24] S. Svelle, C. Tuma, X. Rozanska, T. Kerber, J. Sauer, *J. Am. Chem. Soc.* **2009**, *131*, 816 – 825.
[25] C. Tuma, J. Sauer, *Chem. Phys. Lett.* **2004**, *387*, 388 – 394.
[26] J. P. Perdew, K. Burke, M. Ernzerhof, *Phys. Rev. Lett.* **1996**, *77*, 3865.
[27] *CPMD 3.5.2*, IBM Research Laboratory and MPI für Festkörperforschung, Stuttgart, **1995**–**2001**.
[28] M. Sierka, J. Sauer, *J. Chem. Phys.* **2000**, *112*, 6983 – 6996.
[29] C. Hättig, A. Hellweg, A. Köhn, *Phys. Chem. Chem. Phys.* **2006**, *8*, 1159 – 1169.
[30] S. Grimme, *J. Comput. Chem.* **2006**, *27*, 1787 – 1799.
[31] Transition-state theory; for details, see the Supporting Information.

